

## SPITZER MEASUREMENTS OF ATOMIC AND MOLECULAR ABUNDANCES IN THE TYPE IIP SN 2005AF

RUBINA KOTAK<sup>1</sup>, PETER MEIKLE<sup>2</sup>, MONICA POZZO<sup>2</sup>, SCHUYLER D. VAN DYK<sup>3</sup>, DUNCAN FARRAH<sup>4</sup>, ROBERT FESEN<sup>5</sup>, ALEXEI V. FILIPPENKO<sup>6</sup>, RYAN FOLEY<sup>6</sup>, CLAES FRANSSON<sup>7</sup>, CHRISTOPHER L. GERARDY<sup>2</sup>, PETER A. HÖFLICH<sup>8</sup>, PETER LUNDQVIST<sup>7</sup>, SEPPU MATTILA<sup>9</sup>, JESPER SOLLERMAN<sup>10</sup>, & J. CRAIG WHEELER<sup>11</sup>

*Draft version November 8, 2017*

### ABSTRACT

We present results based on Spitzer Space Telescope mid-infrared (3.6–30  $\mu\text{m}$ ) observations of the nearby IIP supernova 2005af. We report the first ever detection of the SiO molecule in a Type IIP supernova. Together with the detection of the CO fundamental, this is an exciting finding as it may signal the onset of dust condensation in the ejecta. From a wealth of fine-structure lines we provide abundance estimates for stable Ni, Ar, and Ne which, via spectral synthesis, may be used to constrain nucleosynthesis models.

*Subject headings:* supernovae: general — supernovae: individual(SN 2005af, SN 1987A, SN 2004dj)

### 1. INTRODUCTION

Mid-infrared (mid-IR) studies of supernovae (SNe) have been hampered by a combination of several factors: their intrinsic faintness at epochs of interest, the high background at mid-IR wavelengths, and strong terrestrial atmospheric absorption. With the sole exception of the extremely nearby (50 kpc) SN 1987A (Roche et al. 1993; Wooden et al. 1993), this wavelength region has remained out of reach for SN studies. Yet, access to the mid-IR region is important for at least two reasons. First, a large number of fine-structure lines that are sensitive to the details of the explosion physics lie in the 5–40  $\mu\text{m}$  region. These provide robust measurements of element abundances permitting direct comparisons with explosion models. Second, core-collapse SNe (CCSNe) have been proposed to be major sources of dust at high redshifts (e.g., Todini & Ferrara 2001), but even in the local Universe, this hypothesis rests on little direct observational evidence. By monitoring the mid-IR evolution, where warm dust emits most strongly, we have a powerful means by which we can ascertain the epoch of dust condensation, and estimate the amount of fresh dust produced in the ejecta. Alternatively, via mid-IR measurements, we can study the development of an IR echo arising in the pre-existing dusty circumstellar medium, thereby constraining the pre-supernova evolution of the

progenitor (e.g., Meikle et al. 2006).

The improvements in terms of sensitivity and spatial resolution afforded by the Spitzer Space Telescope (*Spitzer*) finally allow us to probe SN behaviour using mid-IR diagnostics. To this end, we are pursuing a multi-epoch spectroscopic and photometric campaign of a significant sample of SNe of all types, within the framework of the Mid-IR Supernova Consortium (MISC). Fortunately, since the launch of *Spitzer*, at least half a dozen CCSNe have exploded within  $\sim 10$  Mpc. Recently, we presented a first mid-IR study of the nearest (3.13 Mpc) of these, SN 2004dj (Kotak et al. 2005). Here, we describe results for the Type IIP SN 2005af that highlight the diversity of this subgroup.

SN 2005af was discovered in the nearby edge-on spiral galaxy, NGC 4945, on 2005 Feb. 8.22 (UT) at  $V = +12.8$  by Jacques & Pimentel (2005). On the basis of a spectrum obtained four days later, Filippenko & Foley (2005) classified it as a Type IIP (plateau) supernova, at an epoch of about one month post-explosion. In what follows, we assume that the supernova exploded on 2005 Jan. 9, but note that the explosion epoch is probably uncertain by up to a few weeks. NGC 4945 is associated with the Centaurus group of galaxies, and estimates of its distance have ranged from 3.9 (de Vaucouleurs et al. 1981) to 8.1 Mpc (Baan 1985). In recent years, these values have tended to converge near the lower end of this range. Following the reasoning in Bergman et al. (1992, and references therein), we adopt a distance of 3.9 Mpc.

### 2. OBSERVATIONS

We first observed SN 2005af with *Spitzer* during Cycle 1 using the Infrared Spectrograph (IRS) and IRS Peak-up Imaging (PUI) under Director's Discretionary Time Program 237. We subsequently observed it during Cycle 2 as part of our GO Program 20256, using the Infrared Array Camera (IRAC), IRS, and IRS-PUI.

#### 2.1. Photometry

3.6–8.0  $\mu\text{m}$  imaging with IRAC was obtained on 2005 Jul. 22 (194 d) and 2006 Feb. 12 (399 d). A frame time of 30 s and 5 (medium-sized) dither positions in mapping mode for each pair of channels were used. Our measurements from aperture photometry, carried out on the

arXiv:astro-ph/0609706v1 26 Sep 2006

<sup>1</sup> ESO, Karl-Schwarzschild Str. 2, Garching-bei-München, D-85748, Germany e-mail: rkotak@eso.org

<sup>2</sup> Astrophysics Group, Imperial College London, Blackett Laboratory, Prince Consort Road, London, SW7 2AZ, U.K.

<sup>3</sup> Spitzer Science Center, 220-6, Pasadena, CA 91125

<sup>4</sup> Department of Astronomy, Cornell University, 106 Space Sciences, Ithaca, NY 14853

<sup>5</sup> Department of Physics and Astronomy, 6127 Wilder Lab., Dartmouth College, Hanover, NH 03755

<sup>6</sup> Department of Astronomy, University of California, Berkeley, CA 94720-3411

<sup>7</sup> Department of Astronomy, Stockholm University, AlbaNova, SE-10691 Stockholm, Sweden

<sup>8</sup> Department of Physics, Florida State University, 315 Keen Building, Tallahassee, FL 32306-4350

<sup>9</sup> Department of Physics and Astronomy, Queen's University Belfast, Belfast BT7 1NN

<sup>10</sup> Dark Cosmology Centre, Niels Bohr Institute, University of Copenhagen, Juliane Maries Vej 30, 2100 Copenhagen Ø, Denmark

<sup>11</sup> Astronomy Department, University of Texas at Austin, Austin, TX 78712

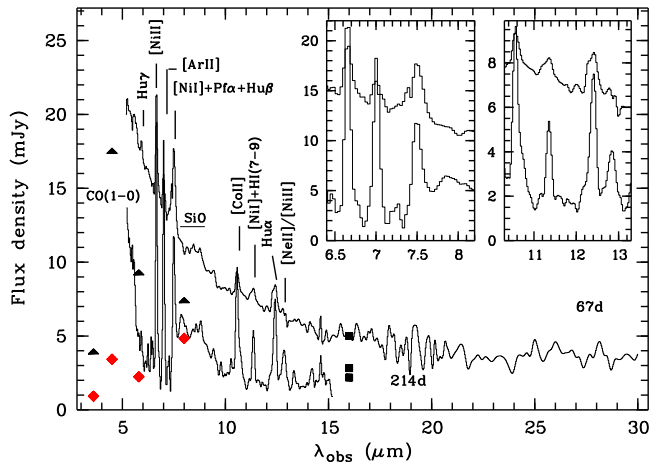


FIG. 1.— Mid-IR spectra of SN 2005af for days 67 (*top curve*) and 214 (*bottom curve*). Plausible line identifications are marked. The IRAC measurements are shown as triangles (194 d) and (red) diamonds (399 d), while the black squares show the PUI measurements for 67, 211, 433 d from top to bottom, respectively. Note the sharp drop in flux between the two IRAC epochs at  $4.5 \mu\text{m}$ , and the relative increase in prominence of the flux at  $\sim 8 \mu\text{m}$ . The IRS flux levels are consistent with the photometry. The insets show the evolution of line profiles described in §3.

post-Basic Calibrated Data, vS14.0.0 image mosaics using GAIA, are shown in Table 1. At 67 d, SN 2005af is very bright in all four IRAC channels. The flux is particularly bright in channel 2 ( $4.5 \mu\text{m}$ ). Nevertheless, examination of individual BCD frames showed that saturation had not occurred i.e. the measurements are robust.

Our first epoch of PUI- $16 \mu\text{m}$  imaging was obtained in Peak-Up mode only, i.e., before dithering capabilities were offered with IRS. The two subsequent epochs of PUI observations were carried out using 31.46 s ramps and 20 small-scale dither positions. The SN was clearly detected at all three epochs (Table 1).

## 2.2. Spectroscopy

Spectra were obtained on 2005 Mar. 17 (67 d) and 2005 Aug. 11 (214 d) with the Short-Low (SL,  $\lambda = 5.2 - 14.5 \mu\text{m}$ ;  $R = 64-128$ ) module of the IRS in staring mode. A Long-Low (LL,  $\lambda = 14 - 38 \mu\text{m}$ ;  $R = 64-128$ ) spectrum was also acquired at 67 d. For the SL mode, the total time-on-source at the two epochs was 1219 s and 1828.5 s respectively, and 629 s for the LL mode.

The first and second epoch data were preprocessed using versions S12.3.0 and S12.4.0, respectively, of the *Spitzer* data processing pipeline. We began the reduction of the BCD data by differencing the two nod positions to remove the background emission. All subsequent steps, i.e., straightening, extraction, wavelength and flux calibration were carried out using SPICE v1.1-beta15 with standard settings. The spectra are shown in Fig. 1. We also extracted the spectra using post-BCD S13.2.0 products and found that they were virtually identical.

## 3. ANALYSIS

The high IRAC flux at  $4.5 \mu\text{m}$  for the first epoch compared to other channels is almost certainly due to CO fundamental band emission. This is corroborated by the steep rise towards  $5 \mu\text{m}$  in both spectra, which we identify with the red wing of the CO fundamental (see Fig. 1). Between 194 d and 399 d, the sharpest decline in IRAC flux is seen at  $4.5 \mu\text{m}$ . These observations suggest that

CO formed in the ejecta less than 2 months after explosion, persisting to at least 7 months, but had faded substantially by about 1 year. The relative increase in the IRAC channel 4 ( $8 \mu\text{m}$ ) flux by 399 d is probably due to the emergence of spectral features in the  $6.43-9.40 \mu\text{m}$  region spanned by this channel. This is discussed below.

By day 214, a pedestal-like feature appears spanning  $\sim 7.6-9 \mu\text{m}$ , which we identify with molecular emission due to the SiO fundamental band (Figs. 1, 3). This is the first time that SiO has been detected in the ejecta of a SN IIP – the most common subtype of all CCSNe at low redshifts. The only other detection of SiO in SN ejecta was in the peculiar Type II SN 1987A (Roche et al. 1991; Wooden et al. 1993). That molecules are detected at all, provides a diagnostic of the prevalent conditions in the ejecta. As both CO and SiO are powerful coolants, they are regarded as precursors to dust condensation in the ejecta (e.g. Nozawa et al. 2003).

In Fig. 2 we compare an LTE model SiO spectrum for SN 1987A at 260 days (Liu & Dalgarno 1994) with the day 214 SL spectrum of SN 2005af. The model, attenuated by a factor of 2.5, produces a convincing reproduction of the observed behaviour. Scaling from the model, the match to our spectrum suggests a SiO mass of  $\sim 2 \times 10^{-4} M_{\odot}$ . Liu & Dalgarno (1994, 1996) argue that such a mass can only form if there is no mixing of helium into the oxygen-silicon region of the ejecta.

Apart from molecular emission, several conspicuous lines are visible in both spectra (Fig. 1) which were identified by analogy with SN 1987A (Wooden et al. 1993). At both epochs, the spectrum is dominated by forbidden lines of Ni, Co, and Ar, of which the [NiII]  $6.64 \mu\text{m}$ , [ArII]  $6.99 \mu\text{m}$ , and [CoII]  $10.52 \mu\text{m}$  are the most prominent.

Between 67 d and 214 d the lines show appreciable increases in intensity (see Table 2, Fig. 1). In addition, in spite of the low spectral resolution ( $R=64-128$ ), we observe in a number of lines (e.g., [NiII]  $\lambda 6.64 \mu\text{m}$ , [CoII]  $\lambda 10.52 \mu\text{m}$ ) an extended red wing at 67 d which fades by 214 d. The broad blend with an extended red wing near  $11.3 \mu\text{m}$  at 67 d is probably due to a combination of [NiI] and HI (7-9), but by 214 d, it is symmetric. Extended red wings were also detected in several lines in SN 1987A (e.g., Witterborn et al. 1989) accompanied by small redshifts of the line centroid. A plausible explanation is provided by electron scattering in the expanding hydrogen envelope (Fransson & Chevalier 1989). This may also apply to SN 2005af, although we do not detect any obvious redshifting of line centroids.

We now estimate the abundances from the stronger lines at the later epoch when the ejecta has a lower optical depth. Following McCray (1990), we estimate the electron density of the ejecta as  $n_e \sim 10^8 t_{\text{yr}}^{-3.5} \text{cm}^{-3} \approx 7 \times 10^8 \text{cm}^{-3}$  at day 214. We derived critical densities for  $\text{Ni}^+$  and  $\text{Ar}^+$  using collision strengths from Bautista & Pradhan (1996) and Osterbrock & Ferland (2006), respectively, and found these to be 1-3 orders of magnitude smaller than  $n_e$ . On this basis, we deem an LTE treatment to be valid. Using the line intensities in Table 2, we derive masses using the upper excited state populations of the ions and find  $3.7 \times 10^{-3} M_{\odot}$ ,  $1 \times 10^{-3} M_{\odot}$ , and  $2.2 \times 10^{-3} M_{\odot}$  for stable ( $\text{Ni}^0, \text{Ni}^+$ ),  $\text{Ar}^+$ , and  $\text{Ne}^+$  respectively, for an electron temperature of 4000 K. Note that the result is insensitive to temper-

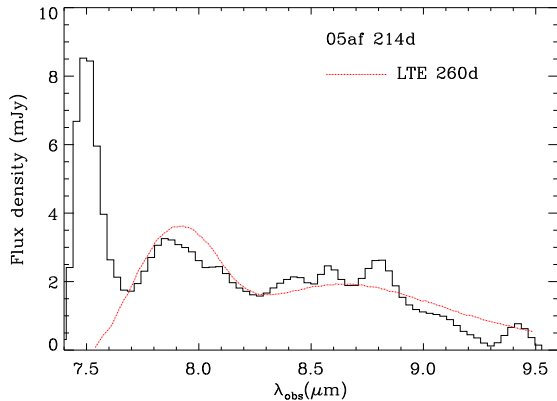


FIG. 2.— The 260 d LTE model from Liu & Dalgarno (1994), attenuated by a factor of 2.5, superimposed on the continuum-subtracted second-epoch spectrum of SN 2005af. From this, we deduce a SiO mass of  $\sim 2 \times 10^{-4} M_{\odot}$  (§3).

ature: a  $\pm 1000$  K change in temperature, changes the mass estimates by  $\lesssim 15\%$ . The partition functions are from Halenka et al. (2001) for Ni, and Irwin (1981) for Ar and Ne. Assuming a uniform distribution of stable Ni, we find that the Sobolev optical depths of all detected Ni lines are less than 0.06. Strong transitions of [NiIII] 11.002  $\mu\text{m}$  and [NiIV] 8.405  $\mu\text{m}$  lie within the wavelength region covered, but these lines are not detected at either epoch. We conclude that the Ni is predominantly in the neutral and singly-ionised state. Thus, assuming insignificant clumping, the value we derive above is probably close to the total stable Ni mass.

The predicted mass of stable Ni is sensitive to the progenitor mass, although this relation is not monotonic, and depends sensitively on the explosion mechanism, multi-dimensional effects and, in spherical models, on the mass cut, which is a free parameter. Thielemann et al. (1996) predict stable Ni masses in the range 0.01–0.014  $M_{\odot}$  for progenitors in the range 13–20  $M_{\odot}$ , and a much lower value of 0.002  $M_{\odot}$  for a 25  $M_{\odot}$  star. Other authors (e.g. Chieffi & Limongi 2004; Woosley & Weaver 1995; Nomoto et al. 2006) derive comparable values, though detailed intercomparisons are difficult due to different parametrizations of physical processes.

Chieffi & Limongi (2004) provide explosive yields as a function of metallicity based on parameters which have been calibrated to fit observed properties of massive stars. The value for the stable Ni mass that we derive is closest to their progenitor models of 13–15  $M_{\odot}$  with metallicities of a third to a twentieth of the solar value. Although we can definitively rule out higher mass progenitors at even lower metallicities, we current cannot exclude a 35  $M_{\odot}$  progenitor at solar metallicity. Further, planned, late-time spectroscopy should provide tighter constraints.

Given the high energy required to ionise neutral Ne (21.6eV) and Ar (15.8eV) we conclude that, given the low ionisation conditions indicated by Ni, the bulk of the Ne and Ar lies in the neutral state. However, no strong transitions of [NeI] or [ArI] lie in our wavelength range. Consequently, the masses derived here for the first ionisation state represent lower limits only.

For SN 1987A at 260 days, using the [CoII] 10.52  $\mu\text{m}$  line, Roche et al. (1993) derive a value for  $M_{\text{Co}^+}$  of 4.6  $\times$

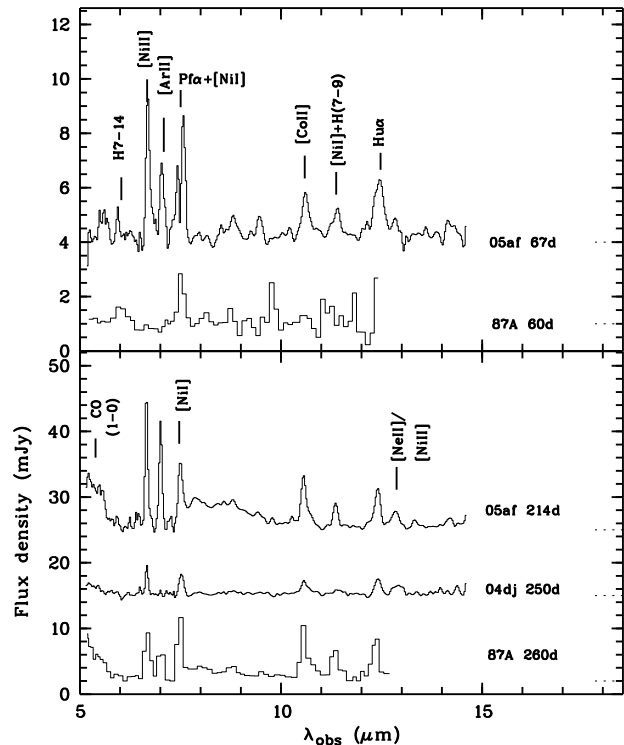


FIG. 3.— Comparison of continuum-subtracted spectra of CC-SNe at roughly coeval epochs. The dotted lines mark the zero-level. Note the striking difference in the strength of the [ArII] line at  $\sim 200$  d between the SNe. The SN 1987A spectra are from Wooden et al. (1993); the 260 d spectrum has been divided by a factor of 5. Isolated features that are common to both epochs are labelled in the top panel only; features that are evident in the later epoch only are indicated in the lower panel. The SN 2004dj spectrum is part of our ongoing monitoring programme; a fuller analysis of these data will be presented elsewhere.

$10^{-3} M_{\odot}$ . Using our day 214 intensity for this line in SN 2005af we obtain  $M_{\text{Co}^+} = 2.4 \times 10^{-3} M_{\odot}$ . Allowing for the different epochs for the two SNe, this implies that a  $^{56}\text{Ni}$  mass of 0.027  $M_{\odot}$  was ejected by SN 2005af. This estimate falls in the expected range for normal Type II SNe (e.g., Hamuy 2003).

Although we have a clear detection of the SN 2005af spectrum between 16–30  $\mu\text{m}$  (Fig. 1) – the first, for any SN at this early epoch – we do not see any significant spectral features. This is not surprising, given its youth. In SN 1987A, lines of [FeII] in this spectral region were only detected after  $\sim 400$  d (Haas 1990).

### 3.1. Comparison with other Type II SNe

In Fig. 3 we compare roughly coeval mid-IR spectra of SN 2005af with that of SN 1987A (IIPec) at  $\sim 60$  d, and with those of SN 1987A and SN 2004dj (IIP) at  $\sim 250$  d. The 60 d mid-IR spectrum of SN 1987A is dominated by HI lines (see Fig. 3 or Roche et al. 1993; Wooden et al. 1993). In contrast, strong lines of [NiII] and [ArII] are present in SN 2005af. This suggests either that our first-epoch SN 2005af observations were taken on the radioactive tail of the lightcurve and that the length of the plateau phase must have been  $\lesssim 60$  d, or that the estimated explosion date, based on the classification spectrum is too late by  $\gtrsim 1$  month.

At the later epoch all three SNe exhibit prominent lines of nickel and cobalt. Wooden et al. (1993) emphasize that the ratio of [NiI] 7.5  $\mu\text{m}$  to [NiII] 6.64  $\mu\text{m}$  lines pro-

vides a sensitive measure of the ionization fraction of Ni ( $\chi_{\text{Ni}} = n_{\text{Ni}^+}/n_{\text{Ni}}$ ). Using their Fig. 9, and assuming LTE, we find  $\chi_{\text{Ni}} \approx 0.35, 0.55$ , and  $0.85$  for SN 2004dj, SN 2005af, and SN 1987A, respectively, at  $\sim 250$  d.

SN 2005af shows much stronger [ArII] than SN 1987A. Moreover, SN 2004dj is found to be a factor of 20 weaker than SN 2005af in this line. Even if we normalise to the strengths of the adjacent [NiII]6.63  $\mu\text{m}$ , [NiI]7.50  $\mu\text{m}$  lines, the [ArII] line is still over  $\times 5$  stronger in SN 2005af. This is intriguing given that SNe 2004dj and 2005af are both of Type IIP. One possibility, indirectly implied by  $\chi_{\text{Ni}}$  above, is that the conditions required to ionize Ar are not attained in SN 2004dj, while  $\text{Ni}^+$ , with its lower ionization potential (7.6eV), is easier to produce.

Another hint may come from the spherically symmetric Thielemann et al. (1996) models, where the bulk of the stable Ar (mostly  $^{36}\text{Ar}$ ) is formed in a shell just above the stable Ni region. Thus, one might expect that a higher mass cut (below which the core collapses to a neutron

star or black hole) within the Ni zone would produce a lower absolute Ni mass, but a higher Ar/Ni mass ratio. However, this seems to be contrary to what we observe, i.e., SN 2004dj has an apparently smaller Ni mass but an even smaller Ar/Ni mass ratio than SN 2005af. We suspect that to account for this behaviour, a certain degree of asymmetry or clumpiness, as well as mixing in the ejecta has to be invoked. Interestingly, Pereyra et al. (2006) infer an overall asphericity of 20% for SN 2005af from optical polarimetry.

This work is based on observations made with the *Spitzer Space Telescope*, which is operated by the Jet Propulsion Laboratory, California Institute of Technology under NASA contract 1407. Financial support for the research is provided by NASA/*Spitzer* grant GO-20256. Support for this work was provided by NASA through an award issued by JPL/Caltech. R.K. and S.M. acknowledge support from an ESO fellowship and from the EURYI Awards scheme respectively.

#### REFERENCES

- Baan, W.A., 1985, *Nature*, 315, 26  
 Bautista, M.A. & Pradhan, A. K., 1996, *A&AS*, 115, 551  
 Bergman, P., et al., 1992, *A&A*, 265, 403  
 Chieffi, A., & Limongi, M., *ApJ*, 2004, 608, 405  
 de Vaucouleurs, G., et al., 1981, *ApJ*248, 408  
 Fransson, C. & Chevalier, R. A., 1989, *ApJ* 343, 323  
 Filippenko, A.V., & Foley, R.J., *IAU Circ.* 8484  
 Halenka, J., Madej, J., et al., 2001, *Acta Astr.*, 51, 347  
 Hamuy, M., 2003, *ApJ*, 582, 905  
 Haas, M.R., et al., 1990, *ApJ* 360, 257  
 Irwin, A.W., 1981, *ApJS*, 45, 621  
 Jacques, C. & Pimentel, E., 2005, *IAU Circ.* 8482  
 Liu, W., & Dalgarno, A., 1994, *ApJ* 428, L769  
 Liu, W., & Dalgarno, A., 1996, *ApJ* 471, L480  
 Kotak, R., et al., 2005, *ApJ*, 628, L123  
 Meikle, W.P.S. et al., 2006, *ApJ* (accepted) astro-ph/0605584  
 McCray, R., 1990, *Molecular Astrophysics*, Cambridge Uni. Press  
 Nomoto, K. et al., 2006, astro-ph/0605725  
 Nozawa, T. et al., 2003, *ApJ*, 598, 785  
 Osterbrock, D.E., & Ferland, G., 2006, *Astrophysics of Gaseous Nebulae and Active Galactic Nuclei*, (University Science Books)  
 Pereyra, A. et al., 2006, *A&A*, 454, 827  
 Roche, P., Aitken, D., & Smith, C., 1991, *MNRAS*, 252, 39P  
 Roche, P., Aitken, D., & Smith, C., 1993, *MNRAS*, 261, 522  
 Thielemann, F.-K., et al. 1996 *ApJ*, 460, 408  
 Todini, P., & Ferrara, A., 2001, *MNRAS*, 325, 726  
 Witteborn, F.C. et al., 1989, *ApJ* 338, L9  
 Wooden, D. et al., 1993, *ApJ* 88, 477  
 Woosley, S.E. & Weaver, T.A., 1995, *ApJS*101, 181

TABLE 1  
PHOTOMETRY OF SN 2005AF

Date	Epoch (d)	$t_{\text{exp}}$ (s)	Flux (mJy)				
			IRAC				PUI
			$3.6\ \mu\text{m}$	$4.5\ \mu\text{m}$	$5.8\ \mu\text{m}$	$8.0\ \mu\text{m}$	$16\ \mu\text{m}$
2005 Mar. 17	67	1219	...	...	...	...	$5.0\pm 0.3$
2005 Jul. 22	194	524	$3.96\pm 0.02$	$17.54\pm 0.04$	$9.31\pm 0.05$	$7.43\pm 0.06$	[3.10]
2005 Aug. 08	211	629	...	...	...	...	$2.83\pm 0.03$
2006 Feb. 12	399	524	$0.93\pm 0.02$	$3.43\pm 0.02$	$2.24\pm 0.02$	$4.84\pm 0.07$	[2.63]
2006 Mar. 18	433	629	...	...	...	...	$2.19\pm 0.03$

NOTE. — Photometry was carried out using a  $5''.5$  radius aperture for all channels. This aperture was chosen to enclose the full diffraction pattern to the first dark ring at the PUI red limit of  $18.7\ \mu\text{m}$ . The aperture was positioned using WCS coordinates. Aperture corrections as appropriate for the outer diffraction rings were applied to IRAC channels 1-4 using Table 5.7 of the IRAC data handbook. No attempt was made to apply a colour correction to the measured PUI fluxes, since the choice of temperature is not obvious. However, we note that the correction would be  $\lesssim 2\%$  for hot dust (500-1000 K), and that such a correction would lie well within our errors. We estimated the systematic error due to variations in the background by repeating our measurements with differing annuli. The errors above are a combination of systematic and statistical errors. The figures in square brackets under the PUI column are indications of the expected fluxes coeval with the IRAC values assuming a  $Q$ -band decline rate similar to that of SN 1987A.  $t_{\text{exp}}$  is the on-source integration time.

TABLE 2  
LINE INTENSITIES

$\lambda_{\text{rest}}$ ( $\mu\text{m}$ )	Ion	Inst.Res. ( $\text{km s}^{-1}$ )	67 d		214 d	
			I	FWHM ( $\text{km s}^{-1}$ )	I	FWHM ( $\text{km s}^{-1}$ )
6.636	[NiII]	2700	3.18	4000	9.42	3600
6.985	[ArII]	2600	1.61	3800	6.16	3000
7.507	[NiI]	2400	...	...	4.48	4000
$10.521^\dagger$	[CoII]	3400	0.78	4500	1.99	3000
$11.308^\ddagger$	[NiI]	3200	0.25	2400	0.78	2900
$12.813^*$	[NeII]	2800	...	...	0.56	3300

NOTE. — The intensities were measured after subtracting a continuum fitted by a low-order polynomial or a spline function; the FWHM were derived from Gaussian fits. Column 3 lists the instrumental resolution; I, the intensity, is in units of  $10^{-14}\ \text{erg cm}^{-2}\ \text{s}^{-1}$ .  $^\dagger$  As this line is symmetric, we assumed that there was no blend with [NiII]  $10.68\ \mu\text{m}$ .  $^\ddagger$  At 67 d this line has a probable contribution from HI(7-9) but by day 214, it is symmetric; above, we assume that it arises due to [NiI] only. Interestingly, the HI(7-9) feature was not detected in SN 1987A at 60 d (Wooden et al. 1993). \* The  $12.8\ \mu\text{m}$  feature at 214 d is likely to be a blend of [NeII]  $\lambda 12.813\ \mu\text{m}$  and [NiII]  $\lambda 12.729\ \mu\text{m}$ . Given the strength of the [NiII]  $6.636\ \mu\text{m}$  line, we estimate that the  $12.8\ \mu\text{m}$  blend comprises roughly equal contributions from the two elements. At 67 d, however, given the strength of the [NiII]  $6.636\ \mu\text{m}$  line, the [NiII]  $12.729\ \mu\text{m}$  line would have been barely detectable.